

See discussions, stats, and author profiles for this publication at: <https://www.researchgate.net/publication/230026024>

# A Fluorescence Study on Swelling of Hydrogels (PAAm) at Various Cross-Linker Contents

ARTICLE *in* ADVANCES IN POLYMER TECHNOLOGY · JANUARY 2010

Impact Factor: 1.05 · DOI: 10.1002/adv.20163

CITATIONS

9

READS

47

## 3 AUTHORS:



**Demet Kaya**

Istanbul Technical University

23 PUBLICATIONS 148 CITATIONS

SEE PROFILE



**Gulsen Akin Evingür**

Piri Reis University

45 PUBLICATIONS 131 CITATIONS

SEE PROFILE



**Önder Pekcan**

Kadir Has University

321 PUBLICATIONS 2,810 CITATIONS

SEE PROFILE

---

# A Fluorescence Study on Swelling of Hydrogels (PAAm) at Various Cross-Linker Contents

---

DEMET KAYA AKTAŞ, GÜLŞEN AKIN EVİNGÜR

*Department of Physics, Istanbul Technical University, Maslak 34398, Istanbul, Turkey*

ÖNDER PEKCAN

*KadirHas University, Cibali 34320, Istanbul, Turkey*

Received: September 11, 2007

Accepted: November 2, 2009

**ABSTRACT:** Disk-shaped acrylamide (AAm) gels were prepared from AAm with various *N,N'*-methylenebisacrylamide (Bis) contents as cross-linker in the presence of ammonium persulfate as an initiator by free-radical cross-linking copolymerization in water. Polyacrylamide (PAAm) gels were dried before using for swelling experiments. Steady-state fluorescence spectrometer was employed during the swelling of PAAm hydrogels in water. Pyranine was introduced as a fluorescence probe. Fluorescence intensity of pyranine from various Bis content gel samples was measured during in situ swelling process. It was observed that fluorescence intensity decreased as swelling has proceeded. Gravimetric and volumetric experiments were also performed. The Li–Tanaka equation was used to determine the swelling time constants,  $\tau_c$ , and cooperative diffusion coefficients,  $D_c$ , from intensity, weight, and volume variations during the swelling processes. It was observed that swelling time constants,  $\tau_c$ , increased and diffusion coefficients,  $D_c$ , decreased as the cross-linker content was increased. © 2010 Wiley Periodicals, Inc. *Adv Polym Techn* 28: 215–223, 2009; Published online in Wiley InterScience (www.interscience.wiley.com). DOI 10.1002/adv.20163

**KEY WORDS:** Diffusion, Fluorescence, Hydrogels, Swelling

*Correspondence to:* Demet Kaya Aktaş; e-mail: demet@itu.edu.tr.

## Introduction

**H**ydrophilic gels, called hydrogels, are cross-linked materials absorbing large quantities of water without dissolving. Hydrogel swelling is directly related to the viscoelastic properties of the gel. The gel elasticity and the friction between the network and solvent play an important role on the kinetics of the gel swelling.<sup>1–3</sup> It has been known that the relaxation time of swelling is proportional to the square of a linear size of the gel,<sup>1</sup> which has been confirmed experimentally.<sup>3</sup> One of the most important features of the gel-swelling process is that it is isotropic. The elastic and swelling properties of permanent networks can be understood by considering two opposing effects, the osmotic pressure and the restraining force. Usually the total free energy of a chemically cross-linked network can be separated into two terms: the bulk and the shear energies. In a swollen network, the characteristic quantity of the bulk free energy is the osmotic bulk modulus,  $K$ . The other important energy, the shear energy, keeps the gel in shape by minimizing the nonisotropic deformation. The characteristic coefficient of these forces is the shear modulus,  $G$ , which can most directly be evaluated by stress–strain measurements.<sup>4,5</sup> Li and Tanaka<sup>6</sup> developed a model in which the shear modulus plays an important role that keeps the gel in shape as a result of coupling of any change in different directions. This model predicts that the geometry of the gel is an important factor and that swelling is not a pure diffusion process.

The equilibrium swelling and shrinking processes of polyacrylamide (PAAm) gels in solvent have been extensively studied.<sup>7–9</sup> It has been reported that acrylamide (AAm) gels undergo continuous or discontinuous volume phase transitions with temperature, solvent composition, pH, and ionic composition.<sup>7</sup> pH-induced volume transitions of AAm gels in an acetone/water mixture were studied using fluorescence technique. When an ionized AAm gel is allowed to swell in water, an extremely interesting pattern appears on the surface of the gel, and the volume expansion increases by adding some amount of sodium acrylate.<sup>9</sup> If AAm gels are swollen in the acetone/water mixture, gel aging time plays an important role during collapse of the network.<sup>9</sup> The kinetics of swelling of AAm gels was studied by light scattering, and the cooperative diffusion coefficient of the network was measured.<sup>1,10</sup> Small-angle X-ray and dynamic light

scattering were used to study the swelling properties and mechanical behavior of AAm gels.<sup>11,12</sup> A pyrene (Py) derivative was employed as a fluorescence probe to monitor the polymerization, aging, and drying of aluminosilicate gels,<sup>13</sup> using the fluorescence technique, where peak ratios in emission spectra were monitored during these processes. The volume phase transitions of PAAm gels were monitored by fluorescence anisotropy and lifetime measurements of densely groups.<sup>14</sup> Steady-state fluorescence (SSF) measurements on swelling of bulk gels formed by free-radical cross-linking copolymerization (FCC) of methyl methacrylate and ethylene glycol dimethacrylate have been reported, where Py was used as a fluorescence probe to monitor swelling process.<sup>15,16</sup> We also reported PAAm hydrogel swelling for various temperatures by using the SSF technique.<sup>17</sup>

In this work, we studied swelling process of PAAm hydrogels at various  $N,N'$ -methylenebisacrylamide (Bis) contents by using SSF technique. The Li–Tanaka equation was used to determine the swelling time constants,  $\tau_c$ , and cooperative diffusion coefficients,  $D_c$ , for the swelling processes. It was observed that swelling time constant,  $\tau_c$ , increased and cooperative diffusion coefficients,  $D_c$ , decreased as the Bis content was increased. Supporting gravimetric and volumetric swelling experiments were also performed by using similar gel samples.

## Theoretical Considerations

It has been suggested<sup>6</sup> that the kinetics of swelling and shrinking of a polymer network or gel should obey the following relation:

$$\frac{W_t}{W_\infty} = 1 - \sum_{n=1}^{\infty} B_n e^{-t/\tau_n} \quad (1)$$

Here  $W_t$  and  $W_\infty$  are the solvent uptakes at time  $t$  and at infinite equilibrium, respectively.  $W_t$  can also be considered as volume differences of the gel between the time  $t$  and zero. Each component of the displacement vector of a point in the network from its final equilibrium location, after the gel is fully swollen, decays exponentially with a time constant  $\tau_n$ , which is independent of time  $t$ . Here  $B_n$  is given

by the following relation<sup>6</sup>:

$$B_1 = \frac{2(3 - 4R)}{\alpha_1^2 - (4R - 1)(3 - 4R)} \quad (2)$$

Here  $R$  is defined as the ratio of the shear and the longitudinal osmotic modulus,  $R = G/M$ . The longitudinal osmotic modulus,  $M$ , is a combination of shear,  $G$ , and osmotic bulk moduli,  $K$ ,  $M = K + 4G/3$ , and  $\alpha_n$  is given as a function of  $R$  as follows:

$$R = \frac{1}{4} \left[ 1 + \frac{\alpha_1 J_0(\alpha_1)}{J_1(\alpha_1)} \right] \quad (3)$$

Here  $J_0$  and  $J_1$  are the Bessel functions.

In Eq. (1),  $\tau_n$  is inversely proportional to the collective cooperative diffusion coefficient,  $D_c$ , of a gel disk at the surface and given by the relation<sup>6</sup>

$$\tau_n = \frac{3a^2}{D_c \alpha_n^2} \quad (4)$$

Here the cooperative diffusion coefficient,  $D_c$ , is given by  $D_c = M/f = (K + 4G/3)/f$ , where  $f$  is the friction coefficient describing the viscous interaction between the polymer and the solvent and  $a$  represents half of the disk thickness in the final infinite equilibrium, which can be experimentally determined.

The series given by Eq. (1) is convergent. The first term of the series expansion is dominant at large  $t$ , which corresponds to the last stage of the swelling. As it is seen from Eq. (4)  $\tau_n$  is inversely proportional to the square of  $\alpha_n$ , where  $\alpha_n$ s are the roots of the Bessel functionals. If  $n > 1$ , then  $\alpha_n$  increases and  $\tau_n$  decreases very rapidly. Therefore, kinetics of swelling in the limit of large  $t$  or if  $\tau_1$  is much larger than the rest of  $\tau_n$ <sup>18</sup>, all high-order terms ( $n \geq 2$ ) in Eq. (1) can be dropped so that the swelling and shrinking can be represented by the first-order kinetics.<sup>18</sup> In this case, Eq. (1) can be written as

$$\frac{W_t}{W_\infty} = 1 - B_1 e^{-t/\tau_c} \quad (5)$$

Eq. (5) allows us to determine the parameters  $B_1$  and  $\tau_c$ .

Here it is important to note that Eq. (5) satisfies the following equation:

$$\frac{dW_t}{dt} = \frac{1}{\tau_c} (W_\infty - W) \quad (6)$$

which suggests that the process of swelling should obey the first-order kinetics. The higher order terms ( $n \geq 2$ ) can be considered as fast decaying perturbative additions to the first-order kinetics of the swelling in the limit of large  $t$ .

## Materials and Methods

Gels were prepared by using 2 M AAm (Merck, Germany) with various Bis (Merck) contents by dissolving them in 25 mL of water in which 2  $\mu$ L of tetramethylethylenediamine was added as an accelerator. The initiator, ammonium persulfate (Merck), was recrystallized twice from methanol. The initiator and pyranine concentrations were kept constant at  $7 \times 10^{-3}$  M and  $4 \times 10^{-4}$  M, respectively, for all experiments. All samples were deoxygenated by bubbling nitrogen for 10 min, just before the polymerization process.<sup>19</sup>

The swelling experiments of disk-shaped PAAM gels were performed at various cross-linker contents. Details of the samples are listed in Table I ( $a_i$ ,  $a_f$ ,  $r_i$ , and  $r_f$  are half thickness and radius of disk shape of gels before and after swelling).

The fluorescence intensity measurements were carried out using the model LS-50 spectrometer of Perkin-Elmer, equipped with a temperature controller. All measurements were made at 90° position, and slit widths were kept at 5 nm. Pyranines in the PAAM hydrogels were excited at 340 nm during in situ swelling experiments. Emission intensities,  $I_{em}$ , of the pyranine were monitored at 427 nm as a function of swelling time. Here, it has to be mentioned that pyranine bonding to PAAM during the FCC causes the blue shift in the emission wavelength of fluorescence intensity of pyranine from 512 to 427 nm.<sup>20</sup> Disk-shaped gel samples were placed on the wall of  $1 \times 1$  quartz cell filled with water for the swelling experiments. The position of the gel and the incident light beam for the fluorescence measurements are shown in Fig. 1 during swelling in water, where  $I_o$  and  $I_{sc}$  are the incident and scattered light intensities, respectively. Here one side of the quartz cell is covered by black cartoon with a circular hole

**TABLE I**  
**Experimentally Measured Parameters of PAAm Hydrogels for Various Bis Content During Swelling Process**

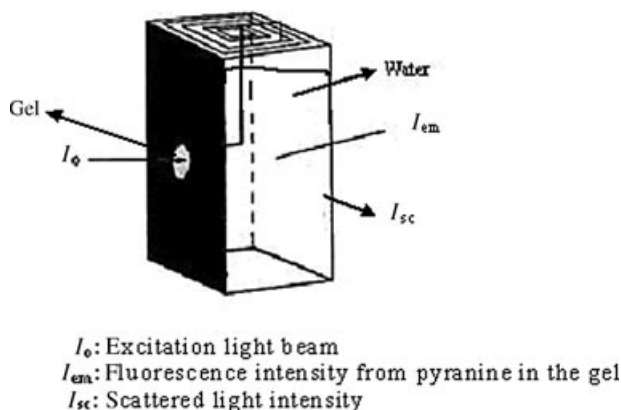
Bis (M)	$a_i \times 10^{-2}$ (m)	$a_f \times 10^{-2}$ (m)	$r_i \times 10^{-2}$ (m)	$r_f \times 10^{-2}$ (m)	$\tau_{cl}$ (min)	$D_{cl} \times 10^{-9}$ (m <sup>2</sup> s <sup>-1</sup> )	$\tau_{cw}$ (min)	$D_{cw} \times 10^{-9}$ (m <sup>2</sup> s <sup>-1</sup> )	$\tau_{cv}$ (min)	$D_{cv} \times 10^{-9}$ (m <sup>2</sup> s <sup>-1</sup> )
0.013	0.09	0.16	0.62	0.98	11.42	52.9	37.5	16.1	65	9.3
0.019	0.08	0.15	0.62	0.93	23.0	24.6	50	11.3	70	8.1
0.026	0.07	0.14	0.5	0.9	28.3	17.5	60	8.2	85	5.8
0.032	0.07	0.14	0.48	0.88	29.0	15.9	100	4.6	250	1.8

$a_i$ : Half of the disk-shaped gels thickness in the initial infinite equilibrium;  $a_f$ : half of the disk-shaped gels thickness in the final infinite equilibrium;  $r_i$ : radius of the disk-shaped gels in the initial infinite equilibrium;  $r_f$ : radius of the disk-shaped gels in the final infinite equilibrium;  $\tau_{cl}$ : fluorescence time constant;  $\tau_{cw}$ : gravimetric time constant;  $\tau_{cv}$ : volumetric time constant;  $D_{cl}$ : fluorescence cooperative diffusion coefficient;  $D_{cw}$ : gravimetric cooperative diffusion coefficient;  $D_{cv}$ : volumetric cooperative diffusion coefficient.

to collimate the light beam in order to minimize the effect of changes in the volume.

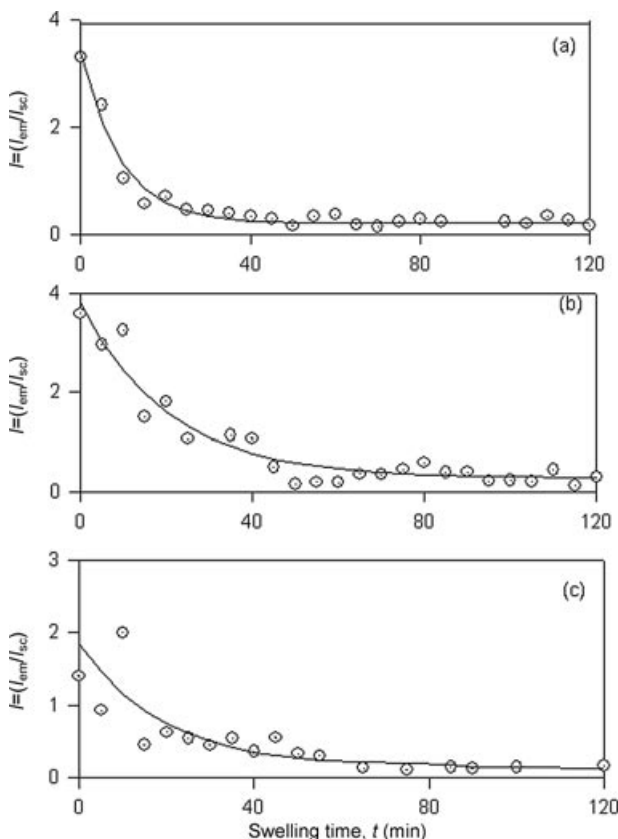
## Results and Discussion

Figure 2a–c show the variations of the corrected pyranine intensities,  $I (= I_{em}/I_{sc})$  of PAAm versus swelling time during hydrogel swelling for 0.013, 0.019, and 0.032 M Bis content samples, respectively. Here scattered intensity,  $I_{sc}$ , is measured at the excitation wavelength 340 nm simultaneously with the emission intensity,  $I_{em}$ , which appears in the same spectra for each swelling step. The reason behind the correction is the variation of turbidity of the gel during the swelling process, which was monitored



**FIGURE 1.** Position of PAAm hydrogel in the fluorescence cell during swelling in water.  $I_0$  is excitation,  $I_{em}$  is emission, and  $I_{sc}$  is scattered light intensities at 340 and 427 nm, respectively.

by using scattered intensity. If gel goes from the heterogeneous to homogeneous state, then scattering light intensity decreases by obeying the Rayleigh model depending on the size of the scattering center. During swelling, any structural fluctuation can



**FIGURE 2.** Corrected fluorescence intensities of pyranine,  $I (= I_{em}/I_{sc})$ , during the swelling process for (a) 0.013 M, (b) 0.019 M, and (c) 0.032 M Bis content samples.

be eliminated by using  $I_{sc}$ , i.e., one has to produce the corrected fluorescence intensity,  $I$ , by dividing emission intensity,  $I_{em}$ , to scattering intensity,  $I_{sc}$ , to eliminate the effect of physical appearance of the gel and produce the meaningful results for the fluorescence quenching mechanisms. It can be observed that as the swelling time,  $t$ , is increased, quenching of excited pyranines increases due to water uptake. It has also to be noted that quenching becomes more efficient at higher cross-linker contents. To quantify these results, the collisional type of quenching mechanism may be proposed for the fluorescence intensity,  $I$ , in the gel sample during the swelling process, where the following relations are given<sup>21</sup>:

$$I^{-1} = I_0^{-1} + k_q \tau_0 [Q] \quad (7)$$

Here,  $k_q$  is the quenching rate constant,  $\tau_0$  is the lifetime of fluorescence probe, and  $Q$  is the quencher.

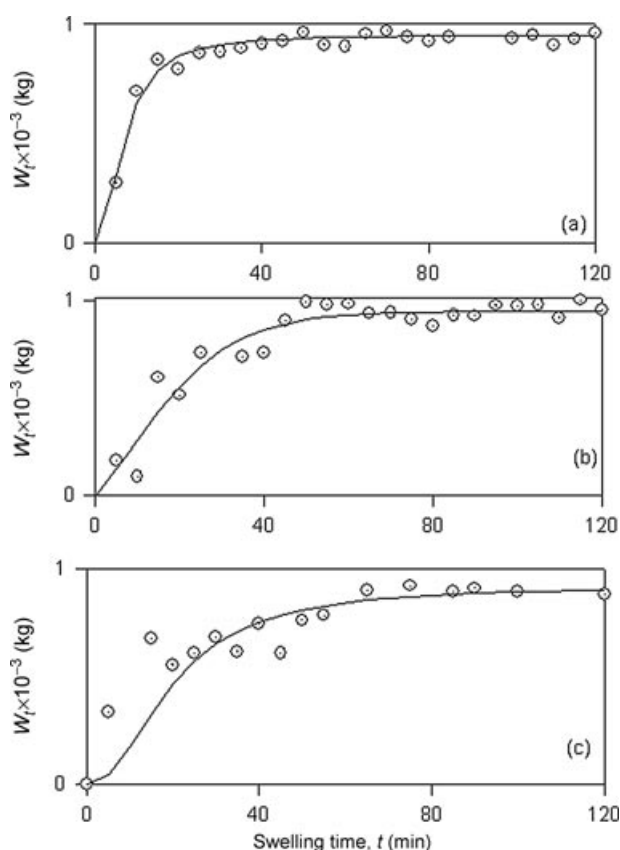


**FIGURE 3.** Plots of water uptake,  $W(t)$ , versus swelling time,  $t$ , for PAAm hydrogels swollen in water for (a) 0.013 M, (b) 0.019 M, and (c) 0.032 M Bis content samples.

For low-quenching efficiency,  $(\tau_0 k_q [Q] \ll 1)$ , Eq. (7) becomes

$$I \approx I_0(1 - k_q \tau_0 [Q]) \quad (8)$$

If one integrates Eq. (8) over the differential volume ( $dv$ ) of the gel from the initial,  $a_0$ , to final,  $a_\infty$ , thickness, and then, reorganization of the relation produces the following useful equation:

$$W = \left(1 - \frac{I}{I_0}\right) \frac{v}{k_q \tau_0} \quad (9)$$

Here water uptake,  $W$ , was calculated over differential volume by replacing  $Q$  with  $W$  as

$$W = \int_{a_0}^{a_\infty} [W] dv \quad (10)$$

where  $v$  is the swollen volume of the gel at the equilibrium swelling, which can be measured

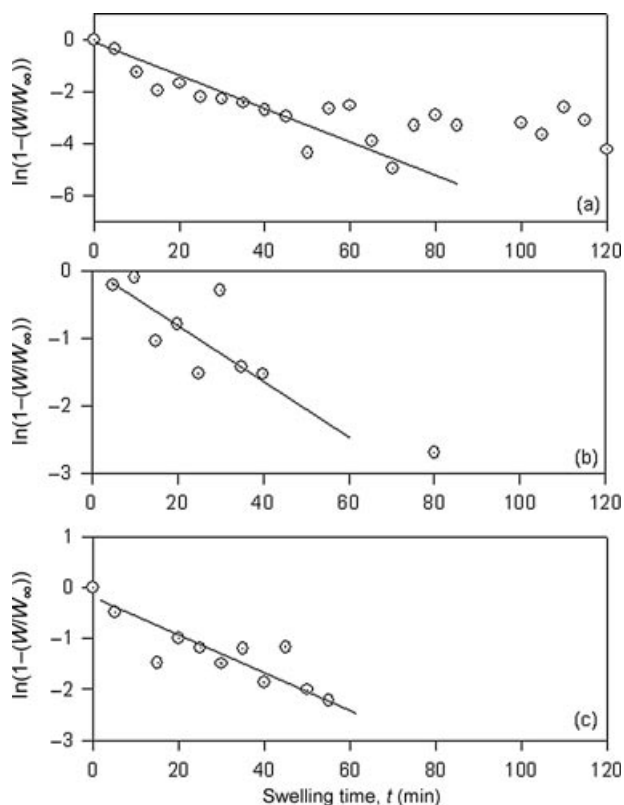


**FIGURE 4.** Fitting of the data in Fig. 3 to Eq. (5) for PAAm hydrogels swollen in water for (a) 0.013 M, (b) 0.019 M, and (c) 0.032 M Bis content samples.

experimentally.  $k_q$  was obtained from separate measurements by using Eq. (9) where the infinity equilibrium value of water uptake,  $W_\infty$  was used for each Bis content sample. Since  $\tau_0$  ( $\approx 5$  ns) is already known from the dry gel, measured values of  $\nu$  can be used to calculate  $k_q$  for each sample separately. The average value of  $k_q$  is found around  $8.28 \times 10^7 \text{ M}^{-1} \text{ s}^{-1}$ . Once  $k_q$  values are measured, the water uptakes,  $W$ , can be calculated from the measured  $\tau$  values at each swelling step. Here, it is assumed that  $k_q$  values do not vary during swelling processes, i.e., the quenching process solely originates from the water molecules.

Plots of water uptake,  $W_t$ , versus swelling time are presented in Fig. 3. The logarithmic forms of the data in Fig. 3 are fitted to the following relation produced from Eq. (5)

$$\ln\left(1 - \frac{W}{W_\infty}\right) = \ln B_1 - \frac{t}{\tau_{cl}} \quad (11)$$

Here,  $\tau_{cl}$  is the time constant measured by the fluorescence technique. Using Eq. (11), linear regressions

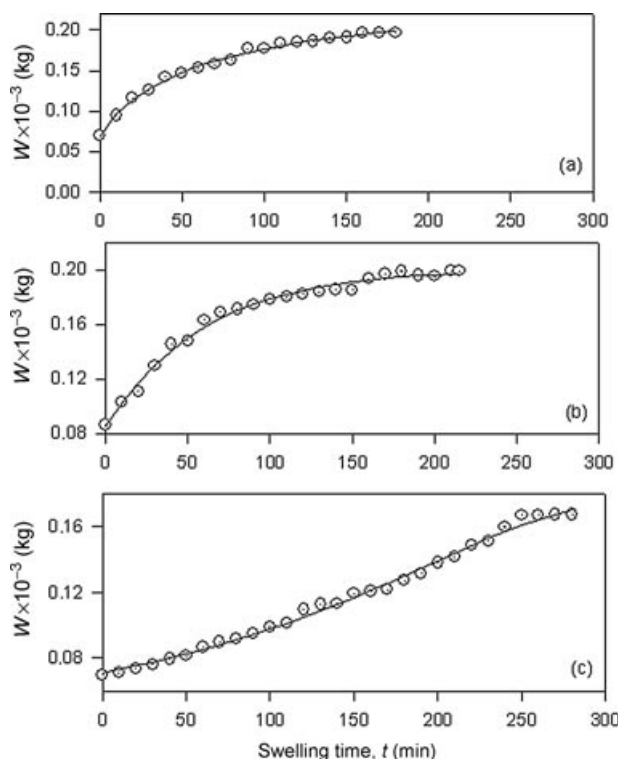


**FIGURE 5.** Plots of the water uptake,  $W$ , measured by gravimetrically, versus swelling time,  $t$ , for PAAm hydrogels swollen in water for (a) 0.013 M, (b) 0.019 M, and (c) 0.032 M Bis content samples.

of curves in Fig. 4 provide us  $B_1$  and  $\tau_{cl}$  values. Taking into account the dependence of  $B_1$  on  $R$ , one obtains  $R$  values and from  $\alpha_1 - R$  dependence  $\alpha_1$  values were produced.<sup>6</sup> Then using Eq. (4), cooperative diffusion coefficients,  $D_c$ , were determined for these disk-shaped hydrogels and found to be around  $10^{-9} \text{ m}^2 \text{ s}^{-1}$ . Experimentally obtained  $\tau_{cl}$  and  $D_{cl}$  values are summarized in Table I, where  $a$  and  $r$  (radius) values are also presented for each gel sample. It should be noticed that  $D_{cl}$  values decrease as the Bis content is increased.

The plots of the solvent uptake,  $W$ , versus swelling time measured by gravimetrically for PAAm hydrogels, swollen in water are shown in Fig. 5. These are typical solvent uptake curves, obeying the Li-Tanaka equation Eq. (5). The logarithmic forms of the data in Fig. 5 are fitted to the following relation produced from Eq. (5):

$$\ln\left(1 - \frac{W}{W_\infty}\right) = \ln B_1 - \frac{t}{\tau_{cw}} \quad (12)$$

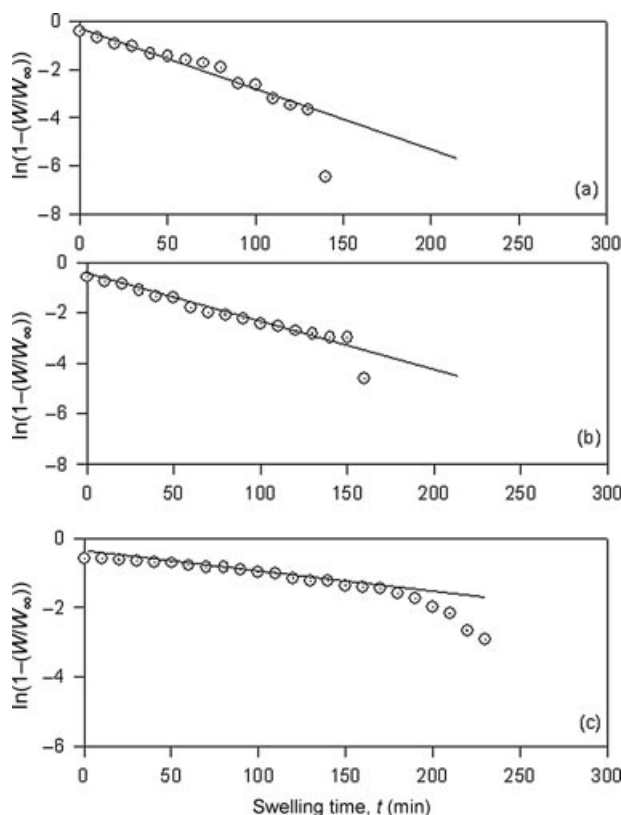


**FIGURE 6.** Linear regressions of the data in Fig. 5 according to Eq. (12) for PAAm hydrogels swollen in water for (a) 0.013 M, (b) 0.019 M, and (c) 0.032 M Bis content samples.

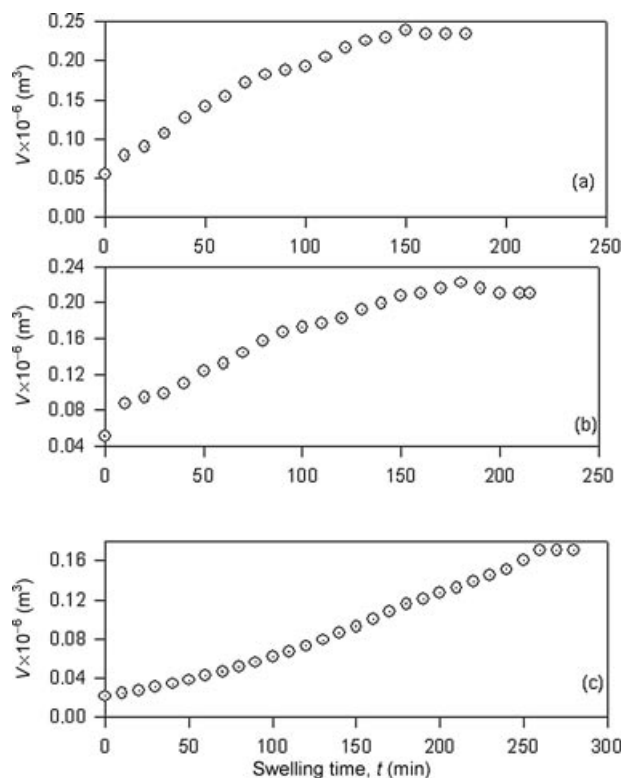


**FIGURE 7.** Plots of the volume,  $v$ , and variation versus swelling time,  $t$ , for PAAm hydrogels swollen in water for (a) 0.013 M, (b) 0.019 M, and (c) 0.032 M Bis content samples.

The fitting of the data is presented in Fig. 6, from which  $B_1$  and gravimetric time constant,  $\tau_{cw}$ , are produced. Then using Eq. (4), gravimetric cooperative diffusion coefficients,  $D_{cw}$ , were determined and are listed in Table I with  $\tau_{cw}$  values. A similar decrease in  $D_{cw}$  is observed as the Bis content is increased.

The variations in volume,  $v$ , of PAAm hydrogels during the swelling process are also measured. The plots of the volume,  $v$ , versus swelling time for PAAm hydrogels, swollen in water are presented in Fig. 7, which are again typical solvent uptake curves, obeying the Li-Tanaka equation Eq. (5). The logarithmic forms of the data in Fig. 7 are fitted to the following relation produced from Eq. (5).

$$\ln\left(1 - \frac{v}{v_\infty}\right) = \ln B_1 - \frac{t}{\tau_{cv}} \quad (13)$$

Here it is assumed that the relation between  $W$  and  $v$  is linear. The fitting of the data is presented in Fig. 8, from which  $B_1$  and  $\tau_{cv}$ , volumetric time constants,

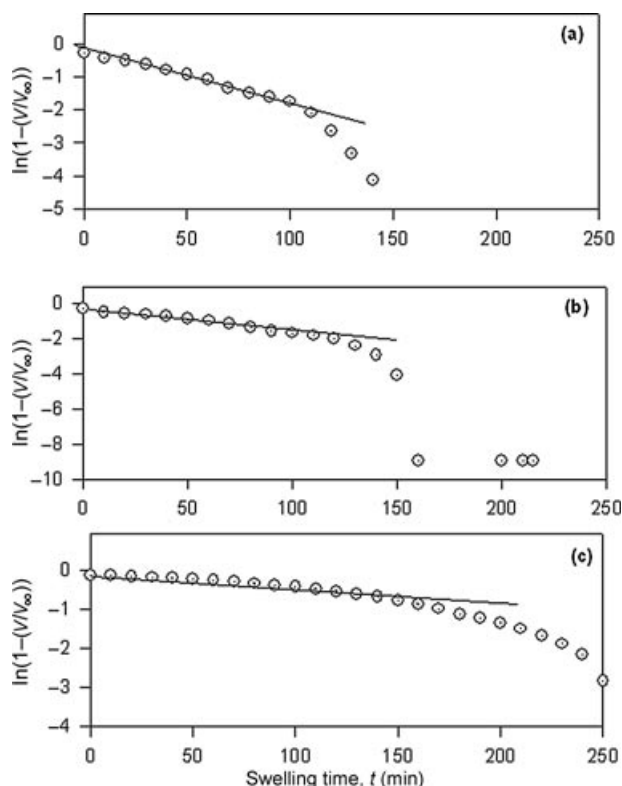


**FIGURE 8.** Linear regressions of the data in Fig. 7 according to Eq. (13) for PAAm hydrogels swollen in water for (a) 0.013 M, (b) 0.019 M, and (c) 0.032 M Bis content samples.

are produced. Then using Eq. (4), volumetric cooperative diffusion coefficients,  $D_{cv}$ , were determined and are listed in Table I with  $\tau_{cv}$  values. Here it is seen in Table I that  $D_c$  values measured by using fluorescence technique are only one order of magnitude larger than the values measured by volumetric and gravimetric techniques, which may present the different behaviors of the gel. It is obvious that the fluorescence technique measures the behavior of the microstructure of the gel, i.e., segmental motion of the gel network can be monitored by using fluorescence intensity because pyranine molecules are bounded to the polymer chains and monitors the swelling at a molecular level. However, volumetric and gravimetric measurements may provide us with the information of the macroscopic behavior (i.e., bulk environment). According to the above-presented argument, one may suggest that chain segments move much faster than the bulk polymeric material during the swelling process. The behavior of the cooperative diffusion coefficients against



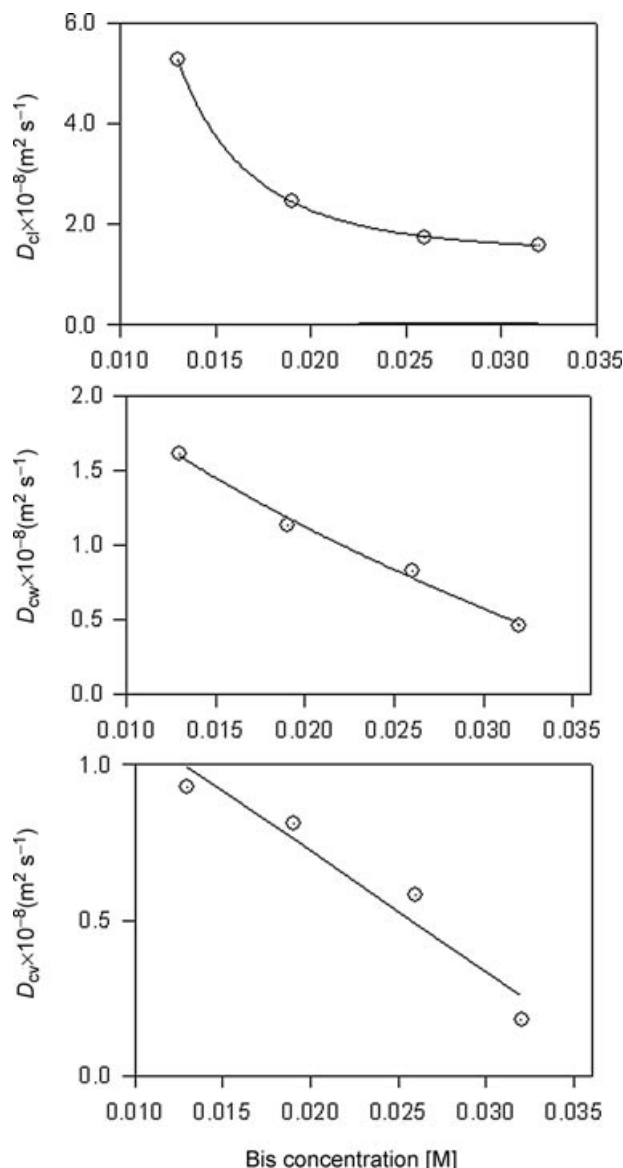


**FIGURE 9.** Cooperative diffusion constants versus Bis content measured by (a) fluorescence, (b) gravimetric, and (c) volumetric techniques.

the Bis content, measured from fluorescence, gravimetric, and volumetric techniques is presented in Figs. 9a and 9b, and c, respectively. It is interesting to note that segmental behavior of  $D_c$  value is exponential; however, macroscopic  $D_c$  values present linear behavior against the Bis content. A similar argument can be raised from the time constant,  $\tau_c$ , values. In other words, segmental motion of the gel seems to be much quicker than the bulk motion of the system.

## Conclusion

These results have shown that the direct fluorescence method can be used for real-time monitoring of the hydrogel swelling process. The Li–Tanaka equation can be used to determine the swelling time constants,  $\tau_c$ , and cooperative diffusion coefficients,  $D_c$ , for the swelling processes. In this method, in situ fluorescence experiments are easy to perform and the cross-linker content was increased with quite sensitive results to measure the swelling parameters in hydrophilic environments.

Several studies related to swelling of polymer hydrogels with various Bis contents have been reported in the literature.<sup>22–24</sup> Hu and others<sup>25</sup> studied the change in microenvironments and dynamics of PAAm gels during the volume phase transition in the acetone/water mixture by measuring the fluorescence spectra, lifetime, and rotational coefficient of a probe. Their results showed that rotational diffusion coefficient decreased as the cross-linker content increased. On the other hand, in our laboratory, the fast transient fluorescence technique (FTRF), which uses the strobe master system (SMS), was employed to study the swelling of disk-shaped PMMA gels and the Li–Tanaka equation was used to determine the cooperative diffusion coefficients,  $D_c$ .<sup>26</sup> FTRF for studying swelling of gels at various cross-linker contents and exposed to organic vapor has been reported.<sup>27</sup> Comparison of gel swelling under organic vapor and in organic solvent was performed using FTRF.<sup>28</sup> Cooperative diffusion constants were found to be in the range of  $(0.37\text{--}4) \times 10^{-9} \text{ m}^2 \text{ s}^{-1}$ , which are considerably smaller than our findings  $(1.8\text{--}52.9) \times 10^{-9} \text{ m}^2 \text{ s}^{-1}$ . The difference between literature values and our findings most probably originates from the solvents at which the gels were swelled. From this one can conclude that  $D_c$  values decreased as the cross-linker content was increased.

## References

1. Tanaka, T.; Filmore, D. *J Chem Phys* 1979, 70, 1214.
2. Peters, A.; Candau, S. J. *Macromolecules* 1986, 19, 1952.
3. Chiarelli, P.; De Rossi, D. *Prog Colloid Polym Sci* 1988, 78, 4.
4. Dusek, K.; Prins, W. *Adv Polym Sci* 1969, 6, 1.
5. Candau, S. J.; Bastide, J.; Delsanti, M. *Adv Polym Sci* 1982, 44, 27.

6. Li, Y.; Tanaka, T. *J Chem Phys* 1990, 92, 1365.
7. Hirokawa, Y.; Tanaka, T. *J Chem Phys* 1984, 81, 6379.
8. Hu, Y.; Horie, K.; Ushiki, H. *Macromolecules* 1992, 25, 6040.
9. Tanaka, T.; Sun, S. T.; Hirokawa, Y.; Katayama, S.; Kucera, J.; Hirose, Y.; Amiya, T. *Nature* 1987, 325, 796.
10. Peters, A.; Candau, S. J. *Macromolecules* 1988, 21, 2278.
11. Ilavsky, M. *Macromolecules* 1982, 15, 78.
12. Patel, S. K.; Rodriguez, F.; Cohen, C. *Polymer* 1989, 30, 2198.
13. Panxviel, J. C.; Dunn, B.; Zink, J. *J Phys Chem* 1989, 93, 2134.
14. Hu, Y.; Horie, K.; Ushiki, H.; Tsunomori, F.; Yamashita, T. *Macromolecules* 1992, 25, 7324.
15. Pekcan, Ö.; Kaya, D.; Erdoğan, M. *Polymer* 2000, 41, 4915.
16. Pekcan, Ö.; Kaya, D.; Erdoğan, M. *J App Poly Sci* 2000, 76, 1494.
17. Aktas, D. K.; Evingür, G. A.; Pekcan, Ö. *J Mater Sci* 2007, 42, 8481.
18. Tanaka, T. *Phys Rev Lett* 1980, 45, 1636.
19. Kaya, D.; Pekcan, Ö.; Yılmaz, Y. *Phys Rev E* 2004, 69, 16117.
20. Yılmaz, Y.; Uysal, N.; Gelir, A.; Guney, O.; Aktaş, D. K.; Gogebakan, S.; Öner, A. *Spectrochim Acta, Part A* 2009, 72, 332.
21. Birks, J. B. *Photophysics of Aromatic Molecules*; Wiley/Interscience: New York, 1971.
22. Ishidao, T.; Akagi, M.; Sugimoto, H.; Iwai, Y.; Arai, Y. *Macromolecules* 1993, 26, 7361.
23. Kayaman, N.; Okay, O.; Baysal, B. *Polym Phys, Part B Polym Phys* 1998, 36, 1313.
24. Peters, A.; Hocquart, R.; Candau, S. J. *Polym Adv Technol* 2003, 2, 285.
25. Hu, Y.; Horie, K.; Ushiki, H.; Yamashita, T.; Tsunomori, F. *Macromolecules* 1993, 26, 1761.
26. Erdogan, M.; Pekcan, Ö. *J Appl Polym Sci* 2003, 87, 464.
27. Erdogan, M.; Yonel, B.; Pekcan, Ö. *Polym Int* 2002, 51, 757.
28. Erdogan, M.; Pekcan, Ö. *Int J Photoenergy* 2005, 7, 37.